

SNEDDS to improve the bioactivities of *Pandanus tectorius* leaves: Optimization, antioxidant, and anticancer activities via apoptosis induction in human cervical cancer cell line

Alifa Husnun Kholieqoh¹, Murni Nur Islamiah Kassim¹, Tengku Sifzizul Tengku Muhammad¹, Khairul Anam², Yeong Yik Sung¹, Hermansyah Amir³, Husna Nugraha Praja⁴, Yosie Andriani^{1*}

¹Institute of Climate Adaptation and Marine Biotechnology, Universiti Malaysia Terengganu, Kuala Nerus, Terengganu, Malaysia.

²Pharmacy Department, Faculty of Medicine, Universitas Diponegoro, Semarang, Indonesia.

³Educational Chemistry Program, Faculty of Teacher Training and Education, University of Bengkulu, Bengkulu, Indonesia.

⁴School of Life Sciences and Technology, Institut Teknologi Bandung, Bandung, Indonesia

ARTICLE HISTORY

Received on: 08/05/2024
Accepted on: 09/09/2024
Available Online: 05/10/2024

Key words:

SNEDDS, cervical cancer, apoptosis, coastal plant, oral bioavailability.

ABSTRACT

Cancer continues to be a deadly disease on a global scale. Furthermore, despite the high expense of their development, synthetic chemotherapeutic drugs currently being used in clinical settings have failed to meet expectations during the past ten years. Therefore, new herbal medications might be alternative anticancer agents that are effective and affordable. Antioxidants in herbs might lessen oxidative stress and prevent carcinogenesis by slowing down and blocking the initiation of cancer cell development. Some researchers have reported that *Pandanus tectorius* has antioxidant activity. However, the antioxidant and anticancer properties of *P. tectorius* leave (PTL) in the form of self-nanoemulsifying drug delivery system (SNEDDS), specifically against human cervical cancer cells (HeLa) have not been studied. This study examined the anticancer activity of PTL-SNEDDS via induction of apoptosis on HeLa cells. All three PTL extracts (hexane, ethyl acetate, and methanol) were successfully formulated into SNEDDS formulation and showed improvement in antioxidant and anticancer activity compared to the crude extract. The cells' morphological characteristics showed that PTL-SNEDDS-treated cells died from both early and late apoptosis. Thus, these findings introduce PTL-SNEDDS as an anticancer agent against human cervical cancer.

INTRODUCTION

Cervical cancer continues to be a significant burden for many nations, particularly for women in developing and underdeveloped nations. The sexually transmitted human papillomavirus (HPV) is the main cause of cervical cancer transmission. Between 2012 and 2016, cervical cancer became the fourth most frequent malignancy in women [1]. In two years, almost 80% of high-risk HPV infections disappear on their own without any treatment [2]. The American Cancer

Society reported that in the United States, there will be 13,960 new cases of invasive cervical cancer diagnosed in women in 2023, and 4,310 of those women will die because of the disease [3].

It is crucial to identify the type of cell death that resulted from the cellular injury for toxicological investigations, dose-response calculations, and diagnostics. Because, it is possible that alterations in cell death could be the initial sign of negative responses to some drugs, such as anticancer drugs. The cellular response to severe injury, including changes that take place before and after cell death must be assessed. Many processes, including apoptosis, necrosis, oncosis, and autophagy can cause cells to die [4]. The size of the cell will shrink if apoptosis is the primary mechanism of cell death, and the plasma membrane will remain intact with the lipids' orientation unaltered. Apoptosis cells may not necessarily

*Corresponding Author
Yosie Andriani, Institute of Climate Adaptation and Marine Biotechnology,
Universiti Malaysia Terengganu, Kuala Nerus, Malaysia.
Email: yosie.hs@umt.edu.my

cause inflammation because phagocytes normally eat them before releasing their contents [5]. Nuclear chromatin condensation, irregular nuclei, and deoxyribonucleic acid (DNA) fragmentation into nucleosome-sized pieces are indications that apoptosis has been triggered in cells [6,7].

Being a common objective of various therapy regimens, apoptosis plays a crucial part in the treatment of cancer [8]. Chemotherapy and chemotherapeutic targeted medicines are the main cancer treatments. Bevacizumab is one of the targeted medicines. It is an angiogenesis inhibitor, which is currently being utilized to treat advanced cervical cancer as an anti-vascular endothelial growth factor monoclonal antibody. Occasionally, this medication is used along with chemotherapy. However, this type of medication may have adverse effects such as fatigue, nausea, and elevated blood pressure. Blood clots, issues with bleeding, poor wound healing, and heart failure are additional less frequent but more severe adverse side effects of Bevacizumab consumption [9]. A carrier for anticancer drugs such as calixarenes is used to reduce their side effects and increase their affinity towards the target [10]. Other research reported that calixarene derivatives, *tert*-butylcalix[4]arene-pyrazole had specific cytotoxicity against the human cervical cancer cells (HeLa) cell line at 2–10 μ M. The compound targeted DNA that was proven by an interaction between ctDNA and the compounds at the air–water interface, thus the compound can be used as a conventional chemotherapeutic agent [11].

Most likely alternative medicine is from natural resources such as plant extracts. Several plants are known to have anticancer properties are widely available, reasonably priced, and have little adverse side effects [12,13]. It is also advised for individuals who have side effects from immunotherapy or chemotherapy to take herbal medications. Herbs with high antioxidant content might lessen oxidative stress in the body caused by free radical species. Antioxidants slow down or stop cell damage, which can inhibit the oxidation process. Antioxidants prevent carcinogenesis by blocking free radicals production, which is the initiation of cancer cell development [14].

The coastal plant, *Pandanus tectorius* is a promising underutilized source to be useful for health. The extracts and two isolated compounds from *P. tectorius* fruit, namely trangeretin and trans ethyl cafeate and its fractions, showed very good activity in inhibiting the activity of the 3-hydroxy-3-methylglutaryl-coenzyme A reductase enzyme [15,16]. Besides that, the alcoholic extract of *P. tectorius* leaves (PTLs) exhibit antioxidant activity [17–19]. However, these bioactivities are probably hindered considering the solubility of the actives extract is less polar or poorly water soluble. Their bioactivity could be higher than the previous investigation. To overcome these problems, a self-nanoemulsifying drug delivery system (SNEDDS) will be one of the most potent delivery methods to improve oral bioavailability and solubility. Some studies on lipid nanotechnology have been formulated successfully and widely reported. However, the application of SNEDDS as the carrier for plant extract is still limited. In the form of SNEDDS, the oral bioavailability of *P. tectorius* leaf extracts could be higher than their original form. The SNEDDS carriers have been proven to improve the antioxidant activity of *P.*

tectorius fruits [20]. Thus, SNEDDS carriers might have the potential to improve the antioxidant and anticancer activity of *P. tectorius* leaf extracts. At present, there is no report on the role of SNEDDS formulations in improving the solubility and anticancer activity of PTLs against human cervical cancer and their apoptosis programmed cell death.

MATERIALS AND METHODS

Plant extraction

PTLs were collected from the Tanjung Gelam area, Terengganu, Malaysia. The leaves were cut and dried at 40°C. 500 g of dried leaves were sequentially extracted using hexane, ethyl acetate, and methanol until the filtrate was clear. The filtrates were evaporated using a rotary evaporator. Then, the yield of extraction was calculated based on the crude extract obtained from each solvent

$$\text{yield (\%)} = \frac{\text{m.crude extract}}{\text{m.dry leave}} \times 100\%$$

New formulation of SNEDDS-loaded PTL extracts

Observation of solubility

Several oils (caprylic triglycerides, olive oil, corn oil, and oleic acid), surfactants (tween 80 and kolliphor RH40), and co-surfactants [PEG 400, dimethyl sulfoxide (DMSO) and propylene glycol] were used to assess the solubility of *P. tectorius* extracts. Each sample was filled into a 1 ml vehicle-filled microtube (Tarson-500020), vortexed, and sonicated in a sonicator bath for one hour at 35°C. Then, a visual evaluation of each sample's solubility was performed [21].

Preliminary screening of surfactant and co-surfactant

Various surfactants and co-surfactants that have passed the solubility test were tested for their emulsifying capacity. Evidence of the easiness of emulsion formation was expressed as the number of flask inversions required to achieve emulsion. The optical clarity of the emulsion was determined spectrophotometrically at 638 nm after the emulsion was allowed to stand for two hours. The emulsion's phase separation was visually observed [22].

Construction of ternary phase diagram

On ternary phase diagrams, oil, surfactant, and co-surfactant were plotted to study phase behavior and track the development of SNEDDS. Water, oil, and Smix (a mixture of surfactant and co-surfactant) were used to represent a point on the triangle in the diagrams, which were created using the aqueous titration method. The self-emulsification region indicated the spontaneous emulsion formation with droplet sizes <200 nm.

Surfactant and co-surfactant were mixed at several weight ratios to construct different ternary phase diagrams. In glass vials, a certain Smix ratio was homogenized after gently mixed with oil at various ratios ranging from 1:9 to 9:1. Distilled water was used to titrate the mixture at room temperature until the endpoint, then visual observation was done to know any phase separation or turbidity. The weight of the water for each addition was noted to create the ternary phase diagram.

CHEMIX School software (version 10.0) was used to construct the ternary phase diagram.

Formulation of PTL-SNEDDS

The PTL-SNEDDS was formulated using the optimized SNEDDS component ratios from the self-emulsifying zone in the ternary phase diagram. Three grams of the optimized SNEDDS formulation are combined with 100 mg of *P. tectorius* and homogenized by gently shaking in a vortex mixer. Then, the mixture was sonicated and heated to 35°C for an hour in an ultrasonicator bath. The prepared PTL-SNEDDS were stored at room temperature in a tightly covered bottle.

Characterization of optimized PTL-SNEDDS formulation

Robustness to dilution

The PTL-SNEDDS formulations were examined for their robustness by dilution 50 and 100 times with distilled water, simulated intestinal fluid (SIF) (pH 7.4), and simulated gastric fluid (SGF) (pH 1.2). The diluted samples were kept for 24 hours while any drug precipitation and phase separation were observed [23,24].

Self-emulsification efficiency time

Briefly, 150 ml of distilled water was gently mixed at 100 rpm with the addition of 0.5 ml of each PTL-SNEDDS formulation. The temperature was adjusted to 37°C ± 0.5°C. The time needed for the SNEDDS to dissolve was recorded. A five-grading system was utilized to assess the easiness of emulsion formation [25].

- Nanoemulsion forms rapidly within one minute with a clear appearance = Grade A.
- Nanoemulsion form within two minutes with slightly less clear or bluish-white appearance = Grade B.
- Fine milky emulsion within two minutes = Grade C.
- Grayish-white emulsion, dull, slightly oily emulsions, take a long time to emulsify (more than two minutes) = Grade D.
- The emulsion was formed in more than three minutes with visible large globules on the surface = Grade E.
- The grades A and B formulations were chosen for further analysis.

Emulsification time deforming

SGF and SIF were used as the medium to study emulsification time deformation [23–26]. The formula for each fluid was:

SGF: 500 ml of a mixture of 1 g NaCl and 33% of HCl (pH 1.2).

SIF: 500 ml of a mixture of 4 g KH₂PO₄ and 0.2N NaOH (pH 7.4).

Emulsification ability was assessed by visual observation. Briefly, 500 µl of each formulation was added into 150 ml of the medium while being gently stirred at 100 rpm and heated to 37°C ± 0.5°C. The time needed for SNEDDS to completely dissolve was recorded. For 4 hours, stable or unstable homogenous emulsions were monitored every 60 minutes.

Thermodynamic stability study

Each PTL-SNEDDS formulation was centrifuged at 3,500 rpm for 30 minutes. A stable formulation with no phase separation was put through a heating–cooling cycle at 45°C and 4°C. PTL-SNEDDS formulations that passed the heating–cooling cycle were put through a freeze–thaw cycle at –21°C and 25°C [26].

Optical clarity

The optical clarity of PTL-SNEDDS that has been emulsified 50 times in distilled water was assessed at 638 nm using a UV-Vis spectrophotometer to know the clarity of nanoemulsion formation as the percentage of transmittance [27].

Droplet size analysis

The droplet size analysis including particle size, zeta potential, and polydispersity index (PDI) of the selected formulation was determined by Particle Size Analyzer (Litesizer 500, Anton Paar). A laser light at $\lambda = 658$ nm was used. Light scattering was monitored at three different angles, 15° (forward scatter), 90° (side scatter), and 175° (back scatter) to measure the particle size and zeta potential. The measurement was done triplicate at 25°C with equilibration time set at two minutes and reported as ±SD. The selected formulation was prepared to 50 times dilutions and gently mixed to ensure homogeneity.

Antioxidant property

Antioxidant activity was assessed by 2,2-diphenyl-1-picrylhydrazyl (DPPH) assay using distilled water and quercetin as negative control and positive control, respectively. The ability of samples as antioxidant were evaluated by the decrease of absorbance at 517 nm as the maximum wavelength for DPPH absorbance measurement using a spectrophotometer UV-1800 (Shimadzu). The absorbance of the sample was measured triplicate and reported as antioxidant activity ±SD. Free radical scavenging activities were calculated by the following equation:

$$\text{Free radical scavenging activity (\%)} = \frac{A_c - A_s}{A_c} \times 100\%$$

where A_s is the absorbance of samples and A_c is the absorbance of negative control [28].

Cell proliferation assay

This assay was using the 3-(4,5-dimethylthiazol-2-yl)-2,5-diphenyltetrazolium bromide (MTT) method. Briefly, HeLa cell (5×10^4 cells/ml equivalent with 5×10^3 cells/well) was seeded in a 96-well plate before treatment and incubated in 5% CO₂ at 37°C for 24 hours. Dissolved samples in RPMI (Roswell Park Memorial Institute) medium were used in various concentrations (from 0.391 to 100 µg/ml). RPMI medium was used as a blank. After 24, 48, and 72 hours, 10 µl of 5 mg/ml MTT solution was put into each well of the plate and incubated for further 4 hours. Then, discard the solution, and 100 µl of DMSO was added into each well and incubated for another 10 minutes to solve the formazan crystals. The absorbance of

the sample was measured at 570 nm (maximum wavelength for MTT absorbance measurement) using a Spark Microplate Reader (TECAN). This assay was done in triplicate and reported as a percentage of cell viability \pm SD. The curves were constructed to obtain IC₅₀ values and the best active fractions.

$$\text{Cell viability (\%)} = \frac{\text{absorbance of sample}}{\text{absorbance of blank}} \times 100\%$$

Morphological features of death cells

The concentration of the sample was prepared based on the IC₅₀ value of each sample. HeLa cell (5×10^4 cells/ml) was seeded in a 96-well plate. The cells were incubated for 24 hours in a 5% CO₂ incubator at 37°C. After 24 hours, the RPMI medium was discarded and replaced with a new medium containing sample and incubated for 4, 8, 20, and 24 hours. The medium was used as the negative control. After incubation, the media was removed and each well was added by Annexin-V/PI reagent. The plates were incubated at room temperature for 5–15 minutes. The ImageXpress Micro XLS Widefield High-Content Analysis System was used to examine the morphological characteristics of cell death.

RESULTS AND DISCUSSION

Plant collection and extraction

The samples were dried to reduce water content. Leaves were extracted by sequential extraction method using three different solvents, hexane, ethyl acetate, and methanol to obtain crude extract for each solvent. The samples were soaked at room temperature for 7–10 days until colorless. Table 1 shows the yield of extracts for each solvent.

New formulation of SNEDDS-loaded *P. tectorius* extracts

Observation of solubility

The observation of the solubility study was intended to know suitable oil phases and surfactants for the development of PTL-SNEDDS. Identifying suitable oil and surfactant/co-surfactant for SNEDDS formulation is very important to optimize drug loading capacity. It shows in Table 2 that *P.*

tectorius methanol extract is insoluble in olive and corn oil. In addition, natural edible oils such as olive and corn oil have a low rate of emulsification and a relatively low drug-loading capacity [29]. Most frequently, medium, and long-chain triglycerides and fatty acids are used as oil to increase the solubility in a formulation.

Preliminary screening of surfactants and co-surfactants

This preliminary screening was done to choose the right surfactant and co-surfactant to give maximum oil-in-water nanoemulsion's thermodynamic stability. By partitioning into the gastrointestinal membrane, surfactants can destabilize the lipid bilayer and exert increased permeability and absorption [29,30]. The effectiveness of emulsification is influenced by a number of variables, including the hydrophilic-lipophilic balance (HLB) value, lipid-surfactant affinity, and the viscoelasticity of the emulsion [30]. All screened surfactants have HLB values of more than 10 because they are suited to produce oil–water nanoemulsions.

Nonionic surfactants are taken into consideration for formulations and pharmaceutical applications because they are less hazardous [31], less affected by changes in pH and ionic strength [32], and typically accepted for oral administration [33]. Oleic acid and caprylic triglycerides were used as the oily phase in a comparison of the emulsification abilities of a few surfactants, including kolliphor RH-40 and tween 80. Table 3 shows the transmittance and number of flask inversions of various combinations of surfactants and co-surfactants.

The results showed that the highest percentage of transmittance (highest emulsification efficiency) for a single oily phase is obtained by a surfactant that has a higher HLB value which is kolliphor RH-40 [HLB value 14–16]. When exposed to water, a more stable nanoemulsion is created when the HLB value is higher [29–32]. In addition, the oils have other impacts. As a medium-chain triglycerides, caprylic triglyceride possesses more solubilizing and self-emulsifying properties [29]. Long chain triglyceride such as oleic acid increase the drug transport in lymph but are sometimes difficult to emulsify [34]. The mixture of oil for the oily phase was also tested in this study. This modification was done to improve pharmacokinetics and meet optimum properties [29].

Table 1. Percentage of crude *P. tectorius* fruits and leaves extracts.

| Sample | Hexane | | Ethyl acetate | | Methanol | |
|--------|------------|----------------|---------------|----------------|------------|----------------|
| | Weight (g) | %Crude extract | Weight (g) | %Crude extract | Weight (g) | %Crude extract |
| PTLs | 14.9115 | 2.71 | 17.0605 | 3.10 | 45.4143 | 8.26 |

Table 2. Observation of solubility of extracts in different kinds of oils, surfactants, and co-surfactants.

| Extract | Oils | | | | Surfactants | | | Co-surfactants | |
|-------------------|-----------|----------|-------------|------------|-------------|----------------|---------|------------------|------|
| | Olive oil | Corn oil | Caprylic TG | Oleic acid | Tween 80 | Kolliphor RH40 | PEG 400 | Propylene glycol | DMSO |
| PTL—Methanol | | | √ | √ | √ | √ | √ | √ | √ |
| PTL—Ethyl acetate | | | √ | √ | √ | √ | √ | √ | √ |
| PTL—Hexane | | | √ | √ | √ | √ | √ | √ | √ |

*√ = miscible

Increased interfacial fluidity, which results from co-surfactants entering the interphase and creating certain vacuum spaces that water can enter, leads to spontaneous emulsification [35]. Co-surfactant reduced the surface tension and allowed it to easily deform around each droplet necessary for the creation of an emulsion [36]. The addition of co-surfactant to water decreases water surface tension, so the surfactant does not feel much stress in the water. Table 4 shows the number of flask

inversions and optical clarity of different mixtures. Propylene glycol demonstrated the highest emulsification efficiency for a single oily phase among the co-surfactants; however, it is more difficult to emulsify than PEG 400. For the use of an oily-phase mixture, the Smix of tween 80 and PEG 400 exhibit great clarity levels and are also easy to emulsify.

Construction of ternary phase diagram

In the absence of extracts, ternary phase diagrams were created to know the self-emulsifying zone and choose an appropriate concentration of each SNEDDS mixture. These diagrams are crucial for understanding the phase behavior of nanoemulsions [22]. Based on the outcomes of the preliminary screening of surfactants and co-surfactants with caprylic triglycerides as the oily phase, kolliphor RH-40 as the surfactant, and propylene glycol as the co-surfactant, a ternary phase diagram was illustrated in Figure 1. In the ternary phase diagram, the nanoemulsion region is shown as a gray area. The system with a Smix ratio (3:2) exhibits a greater emulsification region compared to other systems, as seen in Figure 1, hence it was chosen for further investigation. The current results demonstrated that a transparent and clear system is produced when the oil concentration is between 0% and 25%.

The systems of the mixture oily phase were constructed using a mixture of oleic acid and caprylic triglycerides (1:2), tween 80, and PEG 400 (Fig. 2). Figure 2 shows that the system with the Smix ratio (2:1) exhibits a wider emulsification region than the other systems, so it was chosen for further investigation. The present results in Figure 2 show that transparent and clear systems are created when oil content is 0%–40%, especially in 15%–35%.

These two systems lead to a greater formation of nanoemulsion (higher emulsification region) [37]. The surfactant decreases the surface tension between the oil and aqueous phase by forming a layer of polar and nonpolar components around the oil globule that faces the aqueous solution and absorbs the oil [38]. The self-emulsification process became more spontaneous when surfactant concentration was increased [39]. but some surfactants might lead to the irritation of gastrointestinal epithelium when used as orally administered substances [22,29]. Therefore, the amount of surfactant in SNEDDS formulation must be at a low level. Hence, it is important to formulate the optimized concentration of oil, surfactant, and co-surfactant.

Table 3. The capacity of surfactants to emulsify.

| Oil | Surfactant | HLB value | No. of inversions | %T |
|------------------------------|-----------------|-----------|-------------------|------|
| Oleic acid (OA) | Kolliphor RH-40 | 14–16 | 10 | 66.5 |
| | Tween 80 | 15 | 8 | 51.5 |
| Caprylic triglycerides (CTG) | Kolliphor RH-40 | 14–16 | 4 | 92.4 |
| | Tween 80 | 15 | 3 | 56.2 |
| OA:CTG (1:1) | Kolliphor RH-40 | 14–16 | 21 | 70.1 |
| | Tween 80 | 15 | 8 | 22.5 |
| OA:CTG (1:2) | Kolliphor RH-40 | 14–16 | 26 | 83.7 |
| | Tween 80 | 15 | 17 | 53.3 |
| OA:CTG (2:1) | Kolliphor RH-40 | 14–16 | 23 | 68.6 |
| | Tween 80 | 15 | 7 | 27.3 |

Table 4. Preliminary screening of co-surfactant.

| Oily phase | Surfactant | Co-surfactant | No. of inversions | %T |
|-----------------------|-----------------|------------------|-------------------|------|
| Caprylic triglyceride | Kolliphor RH-40 | PEG 400 | 3 | 34.8 |
| | | Propylene glycol | 7 | 56.3 |
| | | DMSO | 6 | 43.7 |
| OA:CT (1:2) | Kolliphor RH-40 | PEG 400 | 13 | 46.7 |
| | | Propylene glycol | 5 | 76.6 |
| | | DMSO | 15 | 65.3 |
| OA:CT (1:2) | Tween 80 | PEG 400 | 3 | 95.0 |
| | | Propylene glycol | 5 | 57.3 |
| | | DMSO | 8 | 95.5 |

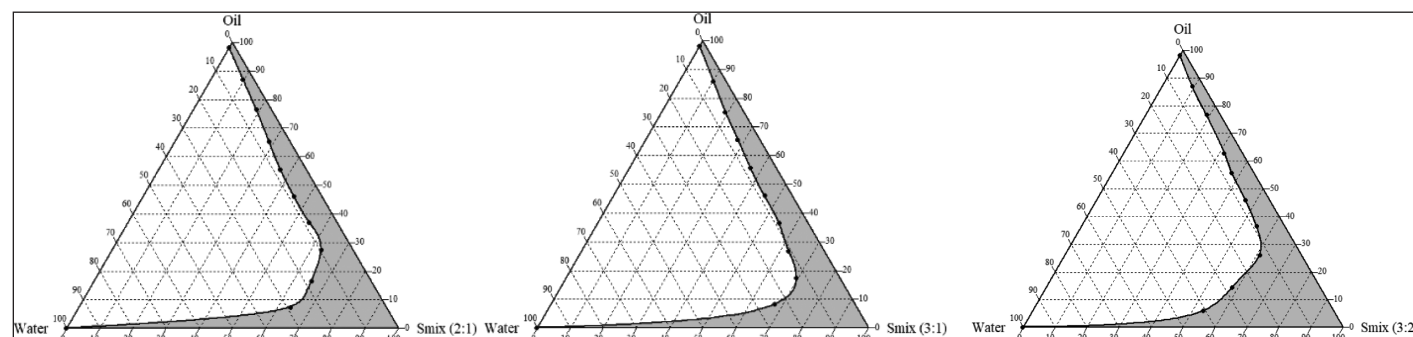


Figure 1. Ternary phase diagrams of caprylic triglycerides, kolliphor RH-40, and propylene glycol at Smix ratios 2:1, 3:1, and 3:2 indicating the clear oil in water nanoemulsion region as gray regions.

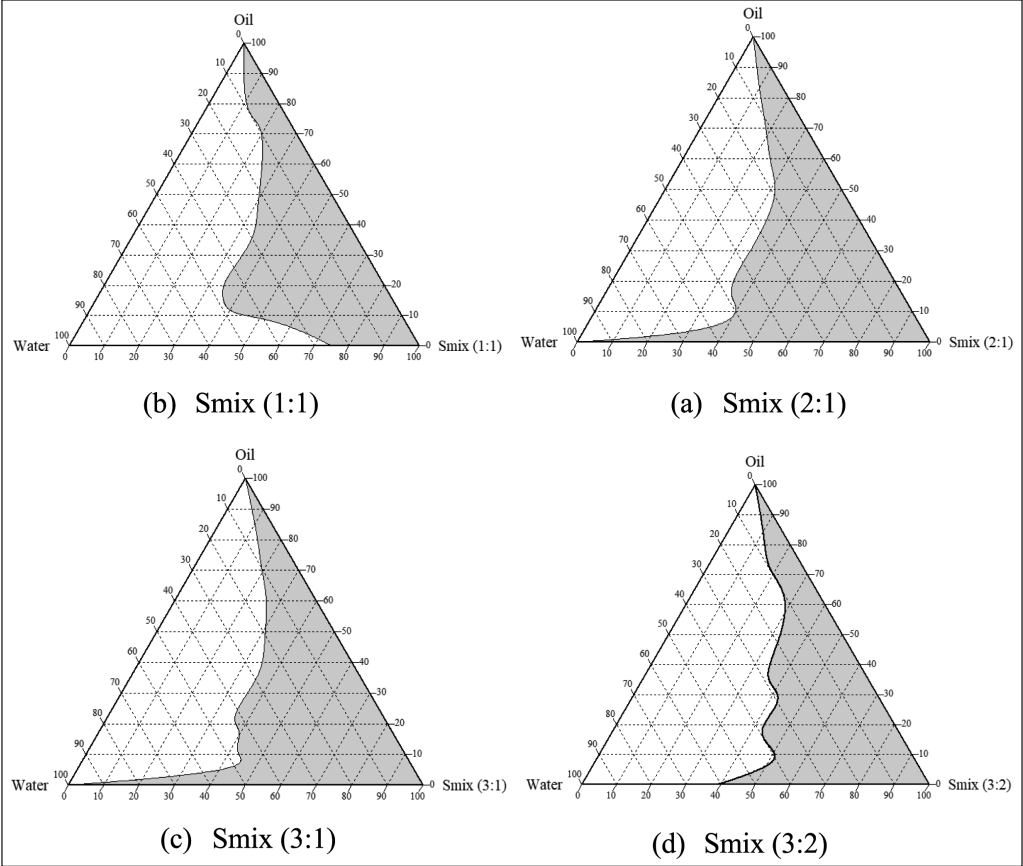


Figure 2. Ternary phase diagrams of the transparent oil-in-water nanoemulsion area are shown as gray regions in the following Smix ratios 1:1, 2:1, 3:1, and 3:2.

Formulation of PTL-SNEDDS

Based on the results from the pseudo-ternary phase diagram (Figs. 1 and 2), formulations of methanol extracts of PTLs-SNEDDS (PTLM-SNEDDS) were made using caprylic triglycerides, kolliphor RH-40, and propylene glycol as the oil phase, surfactant, and co-surfactant, respectively, with the composition of Smix 3:2. For hexane and ethyl acetate extracts of PTLs-SNEDDS (PTLH-SNEDDS and PTLEA-SNEDDS) were made using mixture of oleic acid and caprylic triglycerides (1:2) as the oil phase, tween 80 as surfactant, and PEG 400 as co-surfactant with the composition of Smix 2:1. The composition of the formula is shown in Table 5.

Characterization of optimized PTL-SNEDDS formulation

Robustness to dilution

The ability of SNEDDS to produce dispersion without phase separation and drug precipitation determines the usefulness of SNEDDS as a drug carrier [40]. Based on visual observations (Table 6), PTLM1-5, PTLEA3-5, and PTLH3-6 formulations were clear and transparent, and there are no signs of phase separation or cloudiness upon dilution with distilled water, SGF, and SIF for 50 and 100 times, even after 24 hours. These results confirmed the suitability and the stability of SNEDDS formulation for orally administered drugs, and offer

Table 5. PTL-SNEDDS formulations.

| Code | SNEDDS carrier compositions | | |
|---------|-----------------------------|------------------|---------------------|
| | Oil (%wt) | Surfactant (%wt) | Co-surfactant (%wt) |
| PTLM-1 | 10 | 54 | 36 |
| PTLM-2 | 12 | 53 | 35 |
| PTLM-3 | 14 | 52 | 34 |
| PTLM-4 | 16 | 50 | 34 |
| PTLM-5 | 18 | 49 | 33 |
| PTLM-6 | 20 | 48 | 32 |
| PTLEA-1 | 16 | 56 | 28 |
| PTLEA-2 | 20 | 53 | 27 |
| PTLEA-3 | 25 | 50 | 25 |
| PTLEA-4 | 30 | 47 | 23 |
| PTLEA-5 | 35 | 43 | 22 |
| PTLH-1 | 15 | 57 | 28 |
| PTLH-2 | 20 | 53 | 27 |
| PTLH-3 | 25 | 50 | 25 |
| PTLH-4 | 30 | 47 | 23 |
| PTLH-5 | 35 | 43 | 22 |
| PTLH-6 | 40 | 40 | 20 |

Table 6. Visual assessment of PTL-SNEDDS for their robustness to dilution.

| Code | Observation | | | | | |
|---------|-----------------|-------|--------|--------|-------|-------|
| | Distilled water | | SGF | | SIF | |
| | 50x | 100x | 50x | 100x | 50x | 100x |
| PTLM-1 | C, S | C, S | C, S | C, S | C, S | C, S |
| PTLM-2 | C, S | C, S | C, S | C, S | C, S | C, S |
| PTLM-3 | C, S | C, S | C, S | C, S | C, S | C, S |
| PTLM-4 | C, S | C, S | C, S | C, S | C, S | C, S |
| PTLM-5 | C, S | C, S | C, S | C, S | C, S | C, S |
| PTLM-6 | LC, S | LC, S | LC, S | LC, S | LC, S | LC, S |
| PTLEA-1 | C, S | C, S | DP, US | DP, US | C, S | C, S |
| PTLEA-2 | C, S | C, S | DP, US | DP, US | C, S | C, S |
| PTLEA-3 | C, S | C, S | C, S | C, S | C, S | C, S |
| PTLEA-4 | C, S | C, S | C, S | C, S | C, S | C, S |
| PTLEA-5 | C, S | C, S | C, S | C, S | C, S | C, S |
| PTLH-1 | H, S | H, S | H, US | H, US | H, US | H, US |
| PTLH-2 | H, S | H, S | H, US | H, US | C, S | C, S |
| PTLH-3 | C, S | C, S | C, S | C, S | C, S | C, S |
| PTLH-4 | C, S | C, S | C, S | C, S | C, S | C, S |
| PTLH-5 | C, S | C, S | C, S | C, S | C, S | C, S |
| PTLH-6 | C, S | C, S | C, S | C, S | C, S | C, S |

Notes: C = clear; LC = less clear; H = hazy; M = milky; DP = drug precipitation; S = stable; US = unstable

the potency of a great drug release profile *in vivo* [26,37]. The nano-dispersion capabilities of the dilution's pH 1.2 and 7.4 are unaffected, but stable formulations in different pH will ensure that at intraluminal pH, the globules would pass through the GI tract without phase separation [26].

Self-emulsification efficiency time

Table 7 displays the time it took to produce nanoemulsion and its dispersibility. Distilled water was used to know the grade of the formulation. All the PTLM, PTLEA, and PTLH passed the dispersibility test with grades A and B. These dispersions give clear, slightly less clear dispersion, and rapidly form within one minute. These results will ensure the potential *in vivo* drug release profile [26,37].

Emulsification time deforming

Emulsification time deforming was used to assess the easiness of SNEDDS-generated nanoemulsions in the simulated intestinal and gastric fluid by mild agitation [25,41]. In simulated intestinal and gastric fluid, SNEDDS should typically be able to spread in less than a minute and maintain their nanoemulsion form.

Table 7. PTL-SNEDDS formulations' self-emulsification time.

| Code | Observation | Emulsification time (sec) | Grade |
|---------|-----------------------|---------------------------|-------|
| PTLM-1 | Clear-slightly green | 43.14 | A |
| PTLM-2 | Clear-slightly green | 37.87 | A |
| PTLM-3 | Clear-slightly green | 35.71 | A |
| PTLM-4 | Clear-slightly green | 33.56 | A |
| PTLM-5 | Clear-slightly green | 31.42 | A |
| PTLM-6 | Bluish-slightly green | 48.78 | B |
| PTLEA-1 | Clear-green | 41.35 | A |
| PTLEA-2 | Clear-green | 45.43 | A |
| PTLEA-3 | Clear-green | 34.98 | A |
| PTLEA-4 | Clear-green | 43.75 | A |
| PTLEA-5 | Clear-green | 44.32 | A |
| PTLH-1 | Green-hazy | 47.12 | B |
| PTLH-2 | Green-hazy | 44.65 | B |
| PTLH-3 | Clear-green | 43.50 | A |
| PTLH-4 | Clear-green | 35.85 | A |
| PTLH-5 | Clear-green | 27.34 | A |
| PTLH-6 | Clear-green | 30.80 | A |

Table 8. Emulsification time of PTL-SNEDDS formulations in SIF and SGF.

| Code | Observation | Emulsification time (sec) | |
|---------|-----------------------|---------------------------|-------|
| | | SIF | SGF |
| PTLM-1 | Clear-slightly green | 40.14 | 39.14 |
| PTLM-2 | Clear-slightly green | 36.39 | 34.65 |
| PTLM-3 | Clear-slightly green | 36.18 | 31.99 |
| PTLM-4 | Clear-slightly green | 33.19 | 28.59 |
| PTLM-5 | Clear-slightly green | 30.37 | 23.13 |
| PTLM-6 | Bluish-slightly green | 56.90 | 51.02 |
| PTLEA-1 | Clear-green | 102.91 | 92.15 |
| PTLEA-2 | Clear-green | 87.62 | 81.35 |
| PTLEA-3 | Clear-green | 74.35 | 65.66 |
| PTLEA-4 | Clear-green | 40.91 | 38.76 |
| PTLEA-5 | Clear-green | 33.53 | 35.37 |
| PTLH-1 | Green-hazy | 72.53 | 39.14 |
| PTLH-2 | Green-hazy | 67.65 | 34.65 |
| PTLH-3 | Clear-green | 45.18 | 31.99 |
| PTLH-4 | Clear-green | 41.54 | 28.59 |
| PTLH-5 | Clear-green | 22.91 | 23.13 |
| PTLH-6 | Clear-green | 36.58 | 51.02 |

Based on Table 8, PTLM1-5, PTLEA1-5, and PTLH3-6 were clear. Therefore, these formulations can be used to create PTL-SNEDDS. In addition, there is no aggregation or precipitation, and the systems are stable for 4 hours at 37°C. It suggests that the formulation can remain in the GI tract in the form of nanoemulsion for four hours before it is absorbed [25]. Hence, these formulations were chosen for further study.

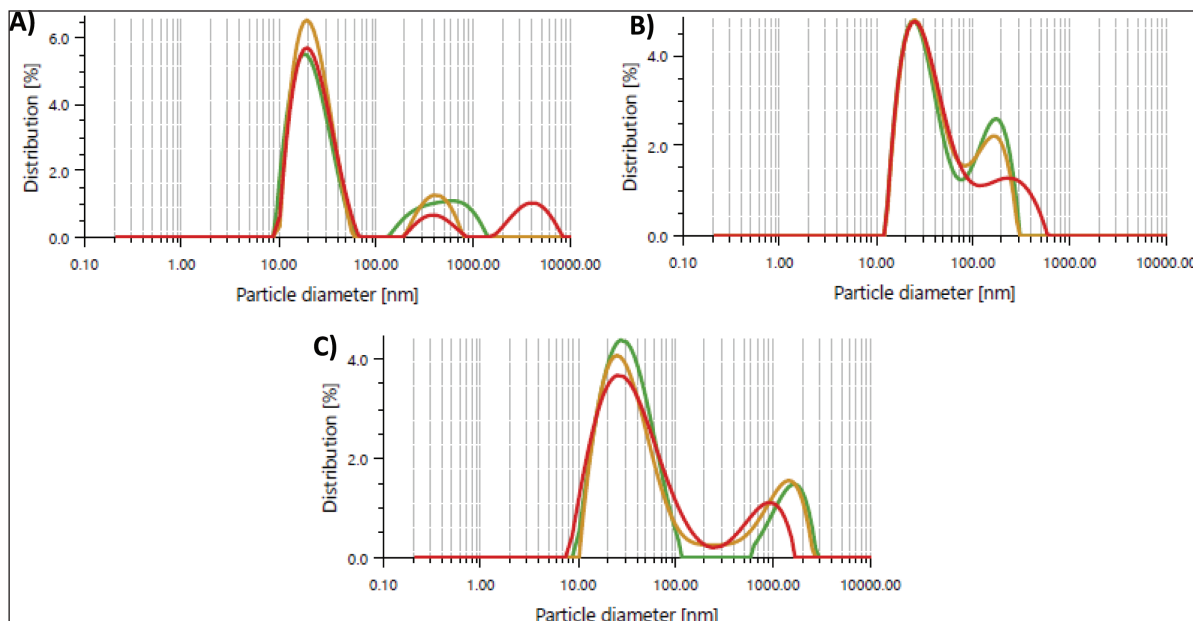


Figure 3. (A) PTLM-SNEDDS, (B) PTLEA-SNEDDS, and (C) PTLH-SNEDDS formulation droplet size graph reconstituted in distilled water.

Thermodynamic stability study

The thermodynamic stability of SNEDDS was determined using different conditions; centrifugation, heating-cooling cycle, and freeze-thaw cycle to know the difference between emulsion and nanoemulsion formation [42] and the stability of the system such as phase separation [43]. All of the formulation with grade A was subjected to this test. The PTLM- 5 and PTLH-3 showed no sign of instability after all of the tests (Table 9). Therefore, these formulations were chosen for the next study.

Optical clarity

The percentage of transmittance showed the clarity level of nanoemulsion. A number of more than 90% for transmittance demonstrates its transparency, lowers the possibility of drug precipitation, and raises the solubilization limit [44]. The outcome provides a prediction for formulation variables such as homogeneity and globule size.

All the optimized formulations exhibit good clarity levels after fifty times dilution in distilled water (Table 10). The PTLM-5, PTLEA-5, and PTLH-3 have a clear-green solution, no cloudiness, milky solution, or substance precipitation. Due to the color, the percentage of transmittance of the PTL formulations is lower than 90%. For PTLM, PTLM-5 was chosen as the best formulation among the two formulations of PTLM because it has a higher content of oil than PTLM-4. Higher oil content and a suitable amount of surfactant created a faster and more stable nanoemulsion [45].

Droplet size analysis

One of the most crucial aspects of a nanoemulsion for assessing stability and a key step in improving medication bioavailability is particle size [46,47]. An increase in drug

Table 9. Thermodynamic stability studies of PTL-SNEDDS formulations.

| Code | Centrifugation | Cycle (@48 hours) | | | | | |
|---------|----------------|-------------------|--------|-------|-------------|--------|-------|
| | | Heating-cooling | | | Freeze-thaw | | |
| | | First | Second | Third | First | Second | Third |
| PTLM-1 | √ | √ | √ | x | - | - | - |
| PTLM-2 | √ | √ | √ | √ | √ | x | - |
| PTLM-3 | √ | √ | √ | √ | √ | x | - |
| PTLM-4 | √ | √ | √ | √ | √ | √ | √ |
| PTLM-5 | √ | √ | √ | √ | √ | √ | √ |
| PTLEA-1 | √ | √ | √ | √ | √ | √ | x |
| PTLEA-2 | √ | √ | √ | √ | x | - | - |
| PTLEA-3 | √ | √ | x | - | - | - | - |
| PTLEA-4 | √ | √ | √ | √ | x | - | - |
| PTLEA-5 | √ | √ | √ | √ | √ | √ | √ |
| PTLH-3 | √ | √ | √ | √ | √ | √ | √ |
| PTLH-4 | x | - | - | - | - | - | - |
| PTLH-5 | x | - | - | - | - | - | - |
| PTLH-6 | x | - | - | - | - | - | - |

Notes. Criteria: phase separation/cracking/cloudiness/precipitation = no, passed (√); yes, failed (x)

Table 10. Clarity level of PTL-SNEDDS formulation.

| Code | Percentage of transmittance (%) |
|---------|---------------------------------|
| PTLM-4 | 97.9 |
| PTLM-5 | 96.7 |
| PTLEA-5 | 31.1 |
| PTLH-3 | 67.3 |

absorption can be caused by smaller particle sizes [48]. The particle size of the optimized formulation is shown in Table 7. The optimized formulations of PTL-SNEDDS have particle sizes lower than 100 nm. The nanometric size lower than 100 nm confirms a larger interfacial surface area for medication absorption. Particle size distribution is shown in Figure 3,

Table 11. Characterization of particle size, PDI, and zeta potential of PT-SNEDDS.

| Code | Particle size (nm) | Zeta potential (mV) | PDI |
|---------|--------------------|---------------------|---------------|
| PTLM-5 | 48.85 ± 2.47 | -20.6 ± 1.0 | 0.218 ± 0.022 |
| PTLEA-5 | 50.73 ± 8.2 | -23.6 ± 0.2 | 0.585 ± 0.041 |
| PTLH-3 | 90.31 ± 7.6 | -44.4 ± 2.2 | 0.256 ± 0.006 |

Table 12. The inhibition of cell proliferation expressed as IC₅₀ value.

| Sample | IC ₅₀ (μg/ml) | | |
|--------------|--------------------------|----------|----------|
| | 72 hours | 48 hours | 24 hours |
| PTLM-SNEDDS | 14.44 | 15.84 | 32.2 |
| PTLEA-SNEDDS | 13.2 | 13.85 | 17.72 |
| PTLH-SNEDDS | 13.56 | 17.85 | 18.94 |

less than 0.7 of the PDI indicates homogenous globule size distribution [46,49,50].

Zeta potential is the difference in potential between the solution's electroneutral area and the surface of a densely bonded layer. The value of zeta potential can be related to the solubility of colloid dispersion. A high zeta potential of small particles confers stability of the dispersion and avoids aggregation [48,49]. The results shown in Table 7 indicate separated emulsion globules and stable systems [51]. Nanoparticles with negative charge can easily permeate the mucus gel compared to positively charged nanoparticles [29]. Among the formulations, PTLH-3 has the highest zeta potential value (-44.4 ± 2.2 mV) as shown in Table 11. This result indicates the low possibility of particle aggregation due to repulsive electrostatic forces [52].

Antioxidant property

The antioxidant activity of all optimized SNEDDS formulations of *P. tectorius* was measured by DPPH scavenging activity. Figure 4 shows that there are differences in antioxidant activity between PTL-SNEDDS and PTL crude extract. All samples exhibit inhibition against DPPH mean oxidation except the hexane extract of PTL because it is a nonpolar fraction and could not dissolve in the solvent (distilled water) that

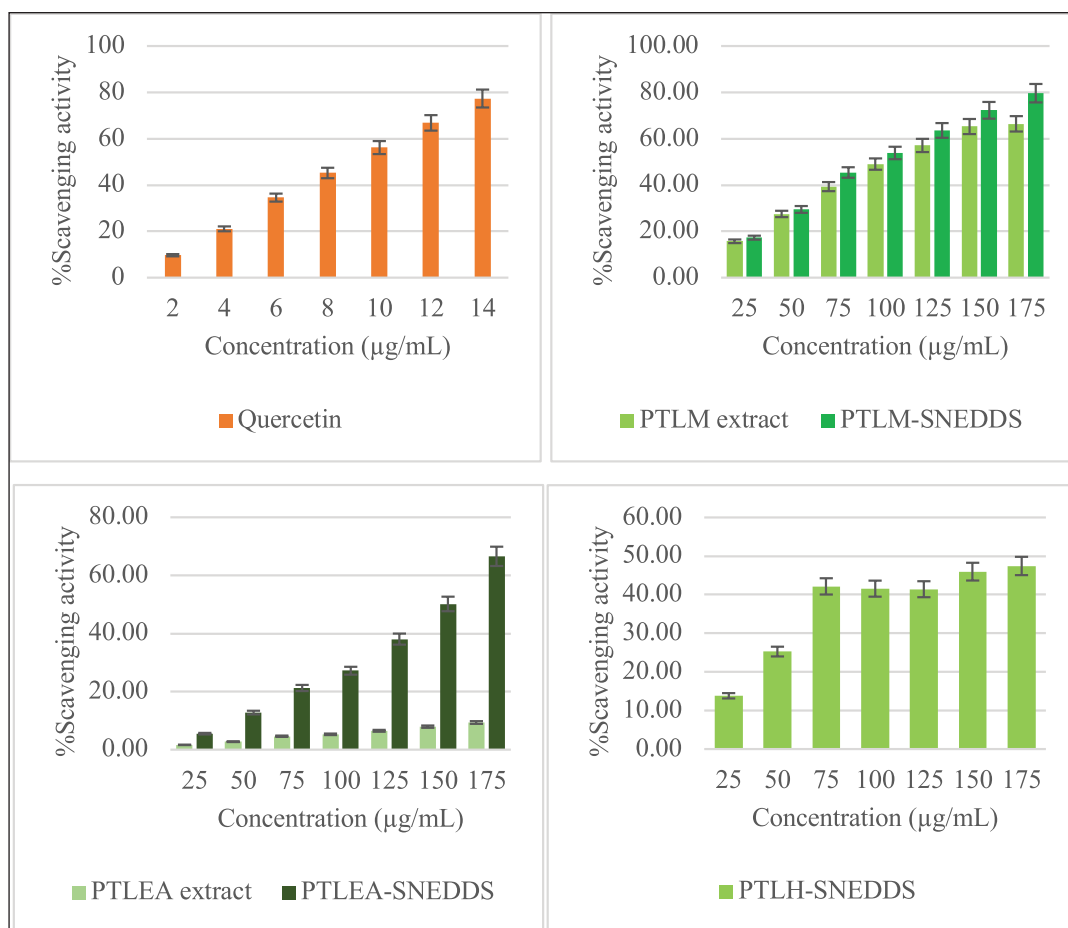


Figure 4. DPPH scavenging activity ± SD of quercetin standard, crude extract, and optimized formulation of PTLM-SNEDDS, PTLEA-SNEDDS, and PTLH-SNEDDS.

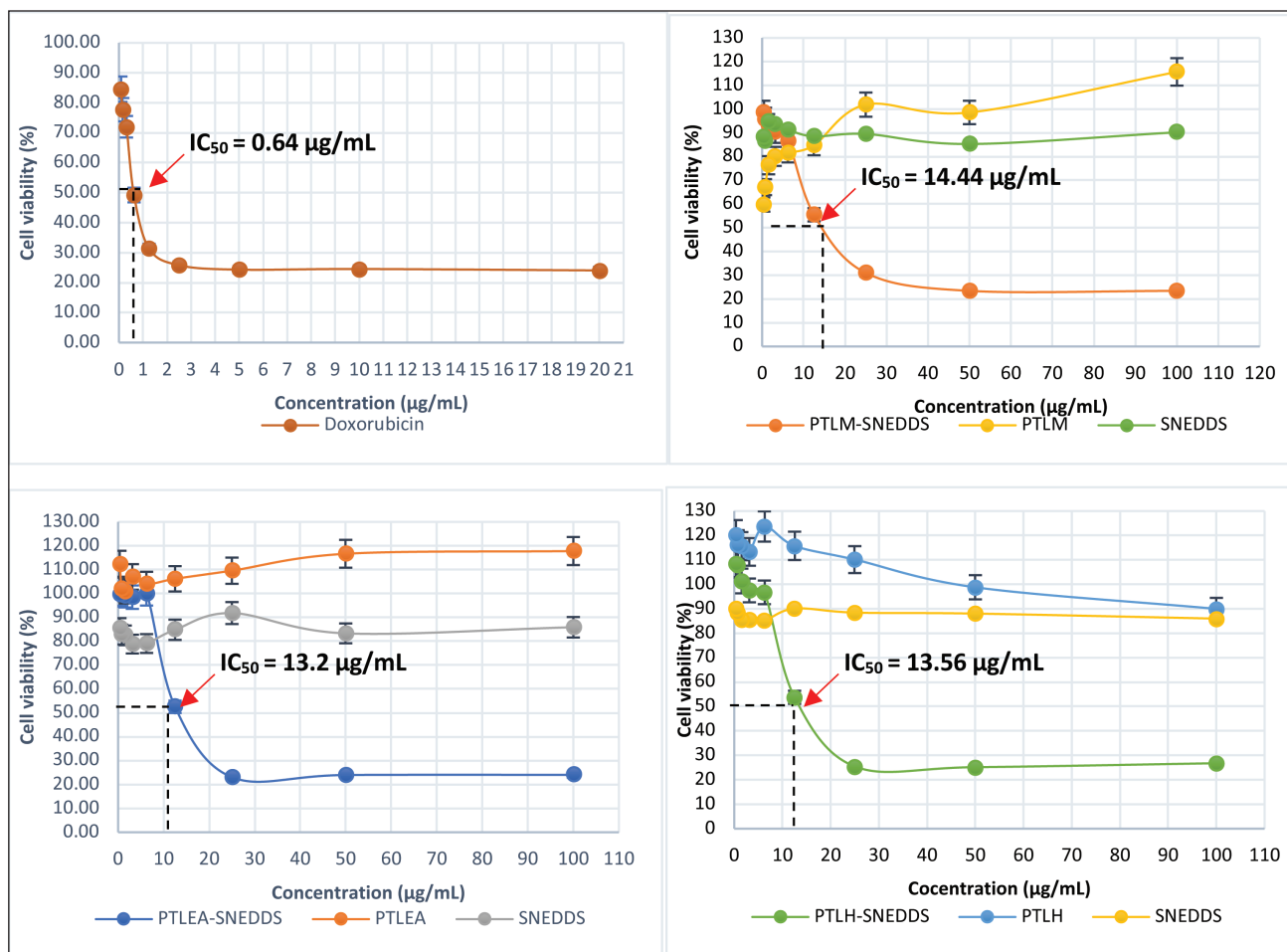


Figure 5. Percentage of growth inhibition \pm SD for Doxorubicin, PTLM, PTLEA, PTLH, SNEDDS carriers, and PTL-SNEDDS against HeLa cells at 72 hours.

has high polarity. The results showed that PTLEA-SNEDDS have greater DPPH scavenging activity about 7 times higher compared to the crude extract. The improvement of scavenging activity of PTLEA-SNEDDS is higher than PTF-SNEDDS [20] and PTLM-SNEDDS due to the polarity of the extract. PTLEA extract is poorly water soluble, so the SNEDDS formulation gave many effects on its solubility and bioactivity in a water solvent. While PTLM has more polar properties than PTLEA, their crude extracts are already soluble in water solvent and only give a little improvement in their solubility and bioavailability. Improvement of antioxidant properties of SNEDDS formulation from fruits part of *P. tectorius* extracts have been investigated but with different compositions of the SNEDDS carrier [20]. Different extracts or samples can be produced from different compositions and ratios of oil, surfactant, and co-surfactant on their SNEDDS formulation. These differences are affected by chemical constituent content in the extracts or sample as well as their polarity will be affected by the formulation result.

Cell proliferation assay

The growth inhibition of all extracts, SNEDDS carrier, and PTL-SNEDDS formulation on HeLa cell lines was investigated. The growth inhibition was determined by

MTT assay and then interpreted as IC_{50} value. The cytotoxicity effect was shown by morphological changes of cells as well as the reduction in the number of viable cells after being treated by sample. The growth inhibition of all samples at 72 hours is shown in Figure 5. The IC_{50} of PTLM-SNEDDS, PTLEA-SNEDDS, and PTLH-SNEDDS were 14.44, 13.2, and 13.56 µg/ml, respectively. According to Andriani et al. [53], the anticancer activity data can be considered cytotoxic if the IC_{50} value is less than 30 µg/ml.

All PTL-SNEDDS formulations are cytotoxic against HeLa cells with IC_{50} value <30 µg/ml. This improvement in cytotoxic property could be correlated to its improvement in antioxidant activity. The propagation of oxidative reaction of free radical species, one of the cancer-causing substances is inhibited by the samples. The growth inhibition was also investigated for all active samples at 24 and 48 hours (Fig. 6).

The PTLM-SNEDDS inhibited the cells' growth at concentrations 15.84 and 14.44 µg/mL at 48 and 72 hours, respectively. At 24 hours, a sample concentration of less than 30 µg/ml is unable to inhibit the growth of the HeLa cell line, only 50 and 100 µg/ml can inhibit $>70\%$ of cell growth. The PTLEA-SNEDDS at 48 with a sample concentration of less than 6.25 µg/ml could not inhibit the growth of HeLa cells.

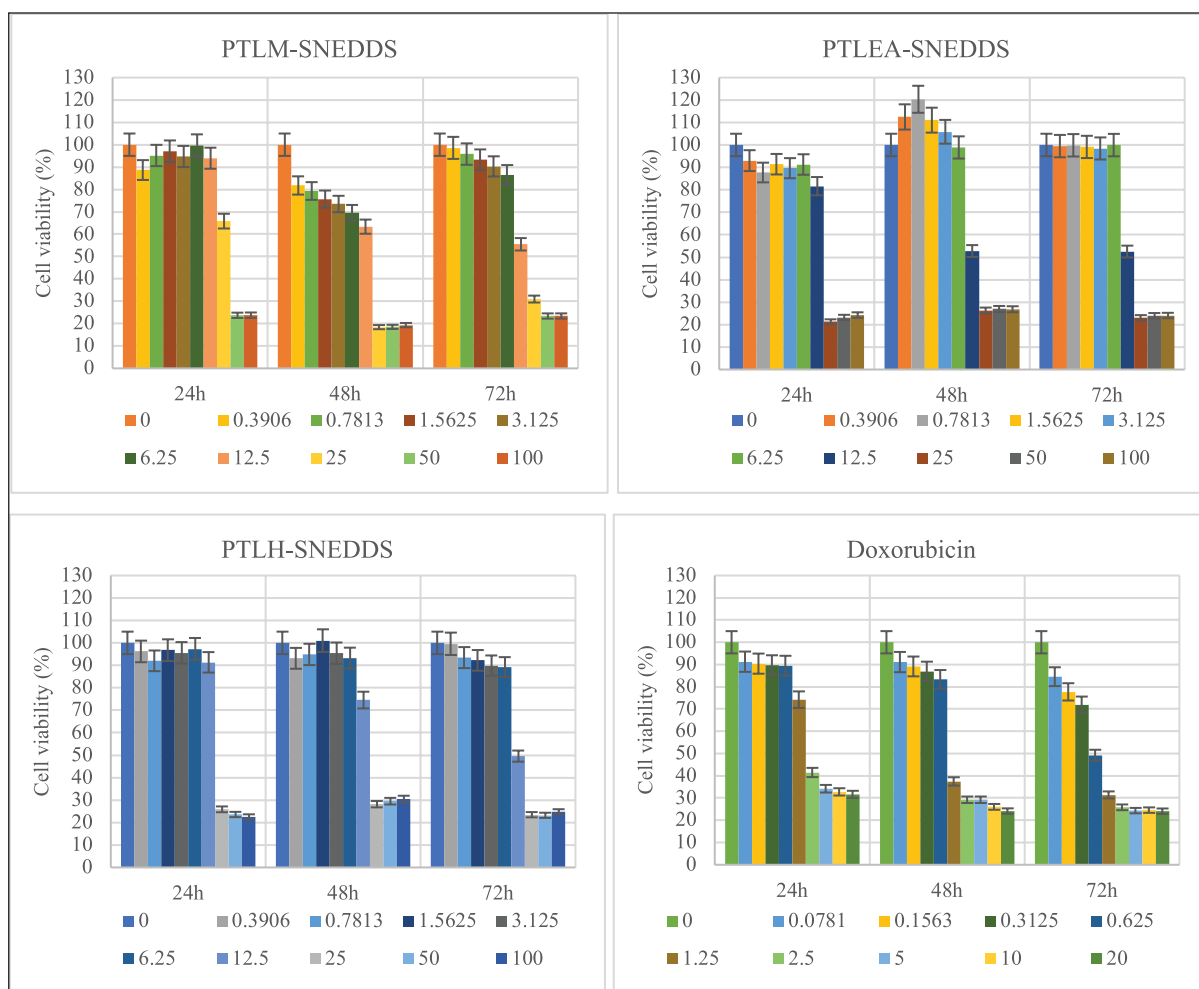


Figure 6. The growth inhibition effects of PTL-SNEDDS and Doxorubicin on HeLa cells at different intervals (24, 48, and 72 hours) and concentrations.

Interestingly, this sample showed a cytotoxicity effect against the HeLa cell line at concentrations 17.72, 13.85, and 13.2 μg/ml at 24, 48, and 72 hours, respectively. The exact same pattern with PTLEA-SNEDDS was observed in the PTLH-SNEDDS sample. At 72 hours, both samples reduced 80% of cell growth at a concentration of 25 μg/ml and had IC_{50} value at 13 μg/ml. The PTLH-SNEDDS produced a cytotoxicity effect against the HeLa cell line at concentrations 18.94, 17.85, and 13.56 μg/ml at 24, 48, and 72 hours, respectively.

For 24, 48, and 72 hours, all the SNEDDS formulations suppress the proliferation of HeLa cells in a dose-dependent manner. Besides that, the IC_{50} values of all samples decreased as the incubation period got longer from 24 to 72 hours.

Morphological features of death cells

The mode of cell death induced by PTLM-SNEDDS, PTLEA-SNEDDS, and PTLH-SNEDDS were done by apoptosis study. The cell was exposed to PTLM-SNEDDS, PTLEA-SNEDDS, PTLH-SNEDDS, and Doxorubicin at IC_{50} value, individually for 72 hours. A common method to monitor the development of apoptosis is the use of Annexin V and fluorescein isothiocyanate (FITC)-conjugated propidium iodide

(PI). The early stage of apoptosis (start-stage) are Annexin V-positive and PI-negative (Annexin V-FITC⁺/PI⁻), compared to late stage of apoptosis cells are Annexin V/PI double positive (Annexin V-FITC⁺/PI⁺) [54].

Figure 7 shows the results acquired after Annexin V/PI tests. From the results, it can be seen that there is a time-dependent effect on cell viability and induces apoptotic morphology in treated cells for 4, 8, 20, and 24 hours (). After 4 hours, PTLM-SNEDDS showed a positive to green stain indicating the early apoptosis cells. While red stain started to appear on cells treated with PTLM-SNEDDS after 8 h of incubation indicating the late apoptosis of the cells. Most of the cells at 24 hours were double-positive to Annexin-V and PI (late apoptosis).

Early apoptosis (green stain) showed on cells treated with PTLEA-SNEDDS at 4 hours, while some of them started to show late apoptosis (red stain). Moreover, after 20 hours, all the cells were double-positive for Annexin-V/PI (late apoptosis). This result showed that late apoptosis started earlier in cells induced by PTLEA-SNEDDS compared to PTLM-SNEDDS. However, the presence of late apoptosis cells that were treated by PTLEA-SNEDDS was less than the PTLH-SNEDDS.

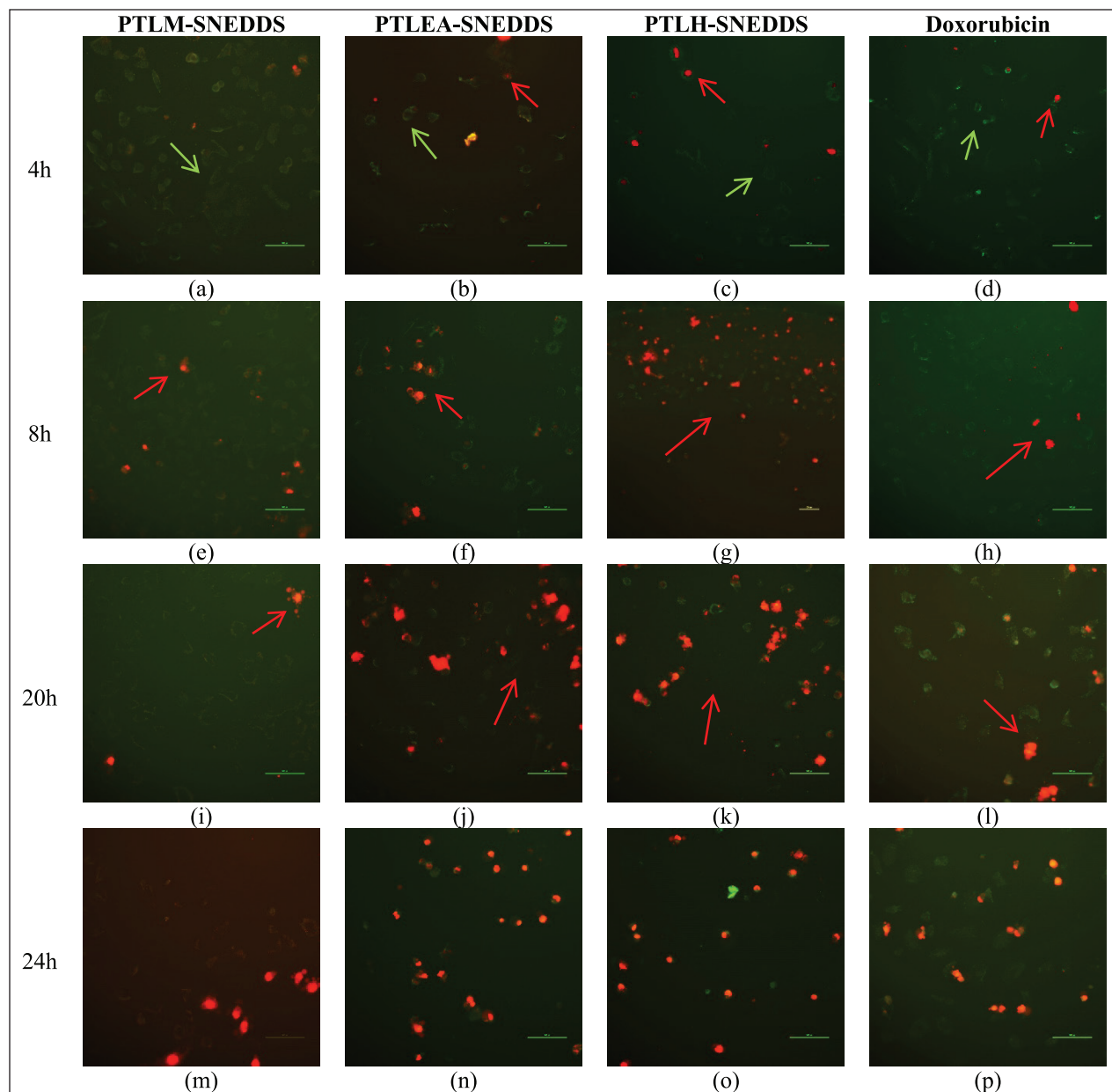


Figure 7. Apoptosis cell death of HeLa cells treated with PTLM-SNEDDS, PTLEA-SNEDDS, PTLH-SNEDDS, and Doxorubicin. The green stain indicates early apoptosis (green arrow), while the red stain indicates late apoptosis (red arrow). The observation was done for 4 hours (a)–(d), 8 hours (e)–(h), 20 hours (i)–(l), and 24 hours (m)–(p).

We can see that the presence of late apoptosis cells in PTLH-SNEDDS was higher than the other samples and the Doxorubicin standard, conducted by the presence of some red stain by PI stain started from 4 hours incubation. At 8 hours and longer, all the cells showed a red stain meaning that late apoptosis had occurred. This result showed that the apoptosis process on cells induced by PTLH-SNEDDS was more rapid compared to other samples and doxorubicin standard.

Apoptosis is referred to as programmed cell death in which a few intracellular enzymatic processes are triggered, causing protein breakdown, and eventual DNA damage. The apoptosis process is observed as cell shrinkage, plasma membrane blebbing, cell separation, nuclear condensation, and

DNA damage [55]. Early apoptosis avoids direct tissue injury because the cell membrane remains intact, preventing the release of the internal components. In addition, phosphatidyl serine (PS) is transported from the inner to the outer layer of the cell membrane during early apoptosis [56]. When the plasma membrane becomes more permeable because of some substances, cells that are in early apoptosis may progress into late apoptosis. Our study showed that PTLM-SNEDDS, PTLEA-SNEDDS, and PTLH-SNEDDS at the concentration of 14.44, 13.2, and 13.56 $\mu\text{g/ml}$, respectively, triggered the transport of PS which indicates the presence of green stain (early apoptosis) start from 4 hours treatment. According to the second study, all SNEDDS samples caused late apoptosis based

on the appearance of red stain after 8 hours after treatment. Correlates with this research, apoptosis-mediated cell death was seen in HeLa after being exposed to SNEDDS formulations of methanol, ethyl acetate, and hexane fraction of PTLs.

CONCLUSION

The SNEDDS of PTLs fractions (methanol, ethyl acetate, and hexane) were successfully formulated into grade A formulations, nanometric size (<100 nm), and PDI lower than 0.7. According to this *in vitro* study, in an aqueous solution, the antioxidant activity of all extracts improved after loading into SNEDDS formulation. Moreover, *P. tectorius* leaf extracts in non-SNEDDS form show no cytotoxic properties against HeLa cells, and interestingly they show anticancer activity in SNEDDS formulations form. The PTL-SNEDDS has the potency as an antioxidant agent and might be an anticancer formulation against HeLa cells. The results of this research showed that SNEDDS formulations can improve solubility and bioactivities of the leaf extracts of *P. tectorius* then will ensure a good prospect as a drug for oral administration.

ACKNOWLEDGEMENT

The authors are thankful for the research support provided by the Fundamental Research Grant Scheme (FRGS) Frasa I 2020/2021 (FRGS/1/2020/STG02/UMT/03/1) of the Ministry of Higher Education (MOHE) of Malaysia.

AUTHOR CONTRIBUTIONS

The authors made substantial contributions to conception and design, data acquisition, data analysis, and interpretation, drafting the manuscript and revising it critically for important intellectual content, and agreed to submit it to the current journal. All the authors are eligible to be an author as per the International Committee of Medical Journal Editors (ICMJE) requirements/guidelines.

CONFLICTS OF INTEREST

The authors report no financial or any other conflicts of interest in this work.

ETHICAL APPROVALS

This study does not involve experiments on animals or human subjects.

DATA AVAILABILITY

All data generated and analyzed are included in this research article.

USE OF ARTIFICIAL INTELLIGENCE (AI)-ASSISTED TECHNOLOGY

The authors declares that they have not used artificial intelligence (AI)-tools for writing and editing of the manuscript, and no images were manipulated using AI.

PUBLISHER'S NOTE

All claims expressed in this article are solely those of the authors and do not necessarily represent those of the

publisher, the editors and the reviewers. This journal remains neutral with regard to jurisdictional claims in published institutional affiliation.

REFERENCES

- Samad SA. Action plan towards the elimination of cervical cancer in Malaysia 2021–2030. 1st ed. Putrajaya, Malaysia: Family Health Development Division, Ministry of Health; 2021. pp 1–68.
- WHO. WHO framework for strengthening and scaling-up services for the management of invasive cervical cancer. 1st ed. Geneva, Switzerland: World Health Organization; 2020. pp 1–114. Available from: <https://www.who.int/publications/i/item/9789240003231>
- ACS. About cervical cancer. *Cervical Cancer*. 2017;2(5):1–9.
- Balvan J, Krizova A, Gumulec J, Raudenska M, Sladek Z, Sedlackova M, *et al.* Multimodal holographic microscopy: distinction between apoptosis and oncosis. *PLoS One*. 2015;10(3):e0121674. <http://doi.org/10.1371/journal.pone.0121674>
- Rock KL, Kono, H. The inflammatory response to cell death. *Annu Rev Pathol Mech Dis*. 2008;3:99–126. <http://doi.org/10.1146/annurev.pathmechdis.3.121806.151456>
- D'Arcy MS. Cell death: a review of the major forms of apoptosis, necrosis and autophagy. *Cell Biol Int*. 2019;43(6):582–92. <http://doi.org/10.1002/cbin.11137>
- Edinger AL, Thompson CB. Death by design: apoptosis, necrosis and autophagy. *Curr Opin Cell Biol*. 2004;16(6):663–9. <http://doi.org/10.1016/j.ceb.2004.09.011>
- Wong RSY. Apoptosis in cancer: from pathogenesis to treatment. *J Exp Clin Cancer Res*. 2011;30(1):1–14. <http://doi.org/10.1186/1756-9966-30-87>
- ACS. Treating cervical cancer. 2021. pp 1–35. Available from: <https://www.cancer.org/content/dam/CRC/PDF/Public/8602.00.pdf>
- Basilotta R, Mannino D, Filippone A, Casili G, Prestifilippo A, Colarossi L, *et al.* Role of calixarene in chemotherapy delivery strategies. *Molecules*. 2021;26(13):3963. <http://doi.org/10.3390/molecules26133963>
- Muravev A, Voloshina A, Sapunova A, Gabdrakhmanova F, Lenina O, Petrov K, *et al.* Calix[4]arene–pyrazole conjugates as potential cancer therapeutics. *Bioorg Chem*. 2023;139:106742. <http://doi.org/10.1016/j.bioorg.2023.106742>
- Khan T, Ali M, Khan A, Nisar P, Jan SA, Afridi S, *et al.* Anticancer plants: a review of the active phytochemicals, applications in animal models, and regulatory aspects. *Biomolecules*. 2020;10(1):47. <http://doi.org/10.3390/biom10010047>
- Lichota A, Gwozdinski K. Anticancer activity of natural compounds from plant and marine environment. *Int J Mole Sci*. 2018;19(11):3533. <http://doi.org/10.3390/ijms19113533>
- Saladin K. Anatomy and physiology: the unity of form and function. New York, NY: McGraw-Hill; 2009. Vol. 53, pp 9.
- Andriani Y, Ramli NM, Syamsumir DF, Kassim MNI, Jaafar J, Aziz NA, *et al.* Phytochemical analysis, antioxidant, antibacterial and cytotoxicity properties of keys and cores part of *Pandanus tectorius* fruits. *Arab J Chem*. 2019;12(8):3555–64. <http://doi.org/10.1016/j.arabjc.2015.11.003>
- Pangestika I, Oksal E, Tengku Muhammad TS, Amir H, Syamsumir DF, Wahid MEA, *et al.* Inhibitory effects of tangeretin and trans-ethyl caffeate on the HMG-CoA reductase activity: potential agents for reducing cholesterol levels. *Saudi J Biol Sci*. 2020;27(8):1947–60. <http://doi.org/10.1016/j.sjbs.2020.06.010>
- Rahayu SE, Sinaga E, Herzagovina S, Jaelani MR. Phytochemical constituents, antioxidant, antibacterial and cytotoxicity properties of *Pandanus tectorius*. *Syst Rev Pharm*. 2019;10(1). <http://doi.org/10.5530/srp.2019.1.45>
- Cheng C, Park SC, Giri SS. Effect of *Pandanus tectorius* extract as food additive on oxidative stress, immune status, and disease resistance in

- Cyprinus carpio*. Fish Shellfish Immunol. 2022;120:287–94. <http://doi.org/10.1016/j.fsi.2021.12.004>
19. Omodamiro O, Ikekemma C. *In vitro* study of antioxidant and anticoagulant activities of ethanol extract of *Pandanus tectorius* leaves. Int Blood Res Rev. 2016;5(1):1–11. <http://doi.org/10.9734/ibr/2016/22231>
 20. Kholieqoh AH, Muhammad TST, Mohamad H, Choukaife H, Seyam S, Alfatama M, *et al.* Formulation and characterization of SNEDDS of *Pandanus tectorius* fruit extract and *in vitro* antioxidant activity. Orient J Chem. 2022;38(4):855–64. <http://doi.org/10.13005/ojc/380404>
 21. Nugroho BH, Syifaudin MR, Fauzi LR, Anggraini E, Ritonga HO. Snedds (self-nanoemulsifying drug delivery system) formulation of sarang semut extract on cervical cancer cells (HeLa) with MTT assay method. J Phys Conf Ser. 2020;1445(1):1–6. <http://doi.org/10.1088/1742-6596/1445/1/012020>
 22. Date AA, Dixit R, Nagarsenker M. Self-nanoemulsifying drug delivery systems: formulation insights, applications and advances. Nanomedicine. 2010;5(10):1595–616.
 23. Abd-Elhakeem E, Teaima MH, Abdelbary GA, El Mahrouk GM. Bioavailability enhanced clopidogrel-loaded solid SNEDDS: development and *in-vitro/in-vivo* characterization. J Drug Deliv Sci Technol. 2019;49:603–14. <http://doi.org/10.1016/j.jddst.2018.12.027>
 24. Sakloetsakun D, Dünhaupt S, Barthelmes J, Perera G, Bernkop-Schnürch A. Combining two technologies: Multifunctional polymers and self-nanoemulsifying drug delivery system (SNEDDS) for oral insulin administration. Int J Biol Macromol. 2013;61:363–72. <http://doi.org/10.1016/j.ijbiomac.2013.08.002>
 25. Wulandari E, Alverina A, Martien R. SNEDDS (self-nanoemulsifying drug delivery system) formulation of B-carotene in olive oil (*Olea europaea*). Int J Adv Res. 2016;4(11):1031–43. <http://doi.org/10.21474/ijar01/2179>
 26. Bhagwat DA, Swami PA, Nadaf SJ, Choudhari PB, Kumbar VM, More HN, *et al.* Capsaicin loaded Solid SNEDDS for enhanced bioavailability and anticancer activity: *in-vitro*, *in-silico*, and *in-vivo* characterization. J Pharm Sci. 2021;110(1):280–91. <http://doi.org/10.1016/j.xphs.2020.10.020>
 27. Akhtartavan S, Karimi M, Karimian K, Azarpira N, Khatami M, Heli H. Evaluation of a self-nanoemulsifying docetaxel delivery system. Biomed Pharmacother. 2019;109:2427–33. <http://doi.org/10.1016/j.biopha.2018.11.110>
 28. Blois MS. Antioxidant determinations by the use of a stable free radical. Nature. 1958;181(4617):1199–200. <http://doi.org/10.1038/1811199a0>
 29. Buya AB, Beloqui A, Memvanga PB, Pr  at V. Self-nano-emulsifying drug-delivery systems: from the development to the current applications and challenges in oral drug delivery. Pharmaceutics. 2020;12(12):1–52. <http://doi.org/10.3390/pharmaceutics12121194>
 30. Kommuru TR, Gurley B, Khan MA, Reddy IK. Self-emulsifying drug delivery systems (SEDDS) of coenzyme Q10: formulation development and bioavailability assessment. Int J Pharm. 2001;212(2):233–46. [http://doi.org/10.1016/S0378-5173\(00\)00614-1](http://doi.org/10.1016/S0378-5173(00)00614-1)
 31. Elnaggar YSR, El-Massik MA, Abdallah OY. Self-nanoemulsifying drug delivery systems of tamoxifen citrate: design and optimization. Int J Pharm. 2009;380(1–2):133–41. <http://doi.org/10.1016/j.ijpharm.2009.07.015>
 32. Constantinides PP. Lipid microemulsions for improving drug dissolution and oral absorption: physical and biopharmaceutical aspects. Pharm Res Official J Am Assoc Pharm Sci. 1995;12(11):1561–72. <http://doi.org/10.1023/A:1016268311867>
 33. Pouton CW, Porter CJH. Formulation of lipid-based delivery systems for oral administration: materials, methods and strategies. Adv Drug Deliv Rev. 2008;60(6): 625–37. <http://doi.org/10.1016/j.addr.2007.10.010>
 34. Chen ML. Lipid excipients and delivery systems for pharmaceutical development: a regulatory perspective. Adv Drug Deliv Rev. 2008;60(6):768–77. <http://doi.org/10.1016/j.addr.2007.09.010>
 35. Dash RN, Mohammed H, Humaira T, Ramesh D. Design, optimization and evaluation of glipizide solid self-nanoemulsifying drug delivery for enhanced solubility and dissolution. Saudi Pharm J. 2015;23(5):528–40. <http://doi.org/10.1016/j.jsps.2015.01.024>
 36. Wang L, Dong J, Chen J, Eastoe J, Li X. Design and optimization of a new self-nanoemulsifying drug delivery system. J Colloid Interface Sci. 2009;330(2):443–8. <http://doi.org/10.1016/j.jcis.2008.10.077>
 37. Kassem AA, Mohsen AM, Ahmed RS, Essam TM. Self-nanoemulsifying drug delivery system (SNEDDS) with enhanced solubilization of nystatin for treatment of oral candidiasis: design, optimization, *in vitro* and *in vivo* evaluation. J Mol Liq. 2016;218:219–32. <http://doi.org/10.1016/j.molliq.2016.02.081>
 38. Lawrence MJ, Rees GD. Microemulsion-based media as novel drug delivery systems. Adv Drug Deliv Rev. 2012;64:175–93. <http://doi.org/10.1016/j.addr.2012.09.018>
 39. Beg S, Swain S, Singh HP, Patra CN, Rao MB. Development, optimization, and characterization of solid self-nanoemulsifying drug delivery systems of valsartan using porous carriers. AAPS PharmSciTech. 2012;13(4):1416–27. <http://doi.org/10.1208/s12249-012-9865-5>
 40. Nasr A, Gardouh A, Ghorab M. Novel solid self-nanoemulsifying drug delivery system (S-SNEDDS) for oral delivery of olmesartan medoxomil: Design, formulation, pharmacokinetic and bioavailability evaluation. Pharmaceutics. 2016;8(3):20. <http://doi.org/10.3390/pharmaceutics8030020>
 41. Suryani S, Zubaydah WOS, Sahumena MH, Adawia S, Wahyuni R, Adjeng ANT, *et al.* Preparation and characterization of self-nanoemulsifying drug delivery system (SNEDDS) from *Moringa oleifera* L. and *Cassia alata* L. leaves extracts. AIP Conf Proc. 2019;2199. <http://doi.org/10.1063/1.5141325>
 42. Syukri Y, Martien R, Lukitaningsih E, Nugroho AE. Novel self-nano emulsifying drug delivery system (SNEDDS) of andrographolide isolated from *Andrographis paniculata* Nees: characterization, *in-vitro* and *in-vivo* assessment. J Drug Deliv Sci Technol. 2018;47(June):514–20. <http://doi.org/10.1016/j.jddst.2018.06.014>
 43. Rahman MA, Iqbal Z, Hussain A. Formulation optimization and *in vitro* characterization of sertraline loaded self-nanoemulsifying drug delivery system (SNEDDS) for oral administration. J Pharm Investig. 2012;42(4):191–202. <http://doi.org/10.1007/s40005-012-0029-0>
 44. Alwadei M, Kazi M, Alanazi FK. Novel oral dosage regimen based on self-nanoemulsifying drug delivery systems for codelivery of phytochemicals—Curcumin and thymoquinone. Saudi Pharm J. 2019;27(6):866–76. <http://doi.org/10.1016/j.jsps.2019.05.008>
 45. Ali HH, Hussein AA. Oral solid self-nanoemulsifying drug delivery systems of candesartan citexetil: formulation, characterization and *in vitro* drug release studies. AAPS Open. 2017;3(1):1–17. <http://doi.org/10.1186/s41120-017-0015-8>
 46. Xi J, Chang Q, Chan CK, MengZY, Wang GN, Sun JB, *et al.* Formulation development and bioavailability evaluation of a self-nanoemulsified drug delivery system of oleanolic acid. AAPS PharmSciTech. 2009;10(1):172–82. <http://doi.org/10.1208/s12249-009-9190-9>
 47. Shakeel F, Haq N, Alanazi FK, Alsarra IA. Polymeric solid self-nanoemulsifying drug delivery system of glibenclamide using coffee husk as a low cost biosorbent. Powder Technol. 2014;256:352–60. <http://doi.org/10.1016/j.powtec.2014.02.028>
 48. Balakumar K, Raghavan CV, Selvan NT, Prasad RH, Abdu S. Self nanoemulsifying drug delivery system (SNEDDS) of Rosuvastatin calcium: design, formulation, bioavailability and pharmacokinetic evaluation. Colloids Surf B Biointerf. 2013;112:337–43. <http://doi.org/10.1016/j.colsurfb.2013.08.025>
 49. Parmar N, Singla N, Amin S, Kohli K. Study of cosurfactant effect on nanoemulsifying area and development of lercanidipine loaded (SNEDDS) self nanoemulsifying drug delivery system. Colloids

- Surf B Biointerf. 2011;86(2):327–38. <http://doi.org/10.1016/j.colsurfb.2011.04.016>
50. Danaei M, Dehghankhold M, Ataei S, Hasanzadeh Davarani F, Javanmard R, Dokhani A, *et al.* Impact of particle size and polydispersity index on the clinical applications of lipidic nanocarrier systems,” *Pharmaceutics*. 2018;10(2):57. <http://doi.org/10.3390/pharmaceutics10020057>
 51. Agrawal AG, Kumar A, Gide PS. Formulation of solid self-nanoemulsifying drug delivery systems using N-methyl pyrrolidone as cosolvent. *Drug Dev Ind Pharm*. 2015;41(4):594–604. <http://doi.org/10.3109/03639045.2014.886695>
 52. Cherniakov I, Domb AJ, Hoffman A. Self-nano-emulsifying drug delivery systems: an update of the biopharmaceutical aspects. *Expert Opinion Drug Deliv*. 2015;12(7):1121–33. <http://doi.org/10.1517/17425247.2015.999038>
 53. Andriani Y, Effendy M, Muhammad TST, Mohamad, H. Antibacterial, radical-scavenging activities and cytotoxicity properties of *Phaleria macrocarpa* (Scheff.) Boerl. leaves in HepG2 cell lines. *Int J Pharm Sci Res*. 2011; 2(7):1700–6.
 54. Brauchle E, Thude S, Brucker SY, Schenke-Layland K. Cell death stages in single apoptotic and necrotic cells monitored by Raman microspectroscopy. *Sci Rep*. 2014;4:4698. <http://doi.org/10.1038/srep04698>
 55. Poon IKH, Hulett MD, Parish CR. Molecular mechanisms of late apoptotic/necrotic cell clearance. *Cell Death and Diff*. 2010;17(3):381–97. <http://doi.org/10.1038/cdd.2009.195>
 56. Wlodkowic D, Telford W, Skommer J, Darzynkiewicz Z. Apoptosis and beyond: cytometry in studies of programmed cell death. *Methods Cell Biol*. 2011;103:55–98.

How to cite this article:

Kholieqoh AH, Kassim MNI, Muhammad TST, Anam K, Sung YY, Amir H, Praja HN, Andriani Y. SNEDDS to improve the bioactivities of *Pandanus tectorius* leaves: Optimization, antioxidant, and anticancer activities via apoptosis induction in human cervical cancer cell line. *J Appl Pharm Sci*. 2024;14(10):175–189.